Journal of the Korean Physical Society, Vol. 68, No. 6, March 2016, pp. 779∼785

Study on the Fabrication of Transparent Electrodes by Using a Thermal-Roll Imprinted Ag Mesh and anATO Thin Film

Sung Jin Kim*
School of Advanced Materials Science and Engineering, Yonsei University, Seoul 03722, Korea, and Icheon Branch, Korea Institute of Ceramic Engineering and Technology, Icheon 17303, Korea

Kyoon Choi
Icheon Branch, Korea Institute of Ceramic Engineering and Technology, Icheon 17303, Korea

Se Young Choi
School of Advanced Materials Science and Engineering, Yonsei University, Seoul 03722, Korea

(Received 29 September 2014, in final form 2 February 2015)

Transparent conductive films have been widely studied because of their potential applications in optoelectronic devices such as paper displays, dye-sensitized solar cells (DSSCs), organic lighting-emitting diodes (OLEDs), organic solar cells and so on. In this paper, we report on a low-resistance, a high-transparents conductive film that can be applied as It a flexible device substrate. In order to the fabricate transparent conductive film, we used a high-resolution roll imprinting method. The following steps were performed: The design and manufacture of an electroforming stamp mold, the fabrication of high resolution roll imprinted on flexible film, and the manufacture of an Ag grid that was filled by using a doctor blade process with a nano-sized Ag paste. Then on patterned Its films, antimony tin oxide was coated with ATO sol solution by using bar the coating method. The fabricated ATO/Ag mesh electrode showed good flexibility, and It exhibited a high optical transmittance of 85.3% in the visible wavelength and a sheet resistance of 41 Ω/sq. Furthermore, the bending test for mechanical properties showed that the ATO/Ag thin film had good flexibility.

PACS numbers: 68.55.-a, 68.55.Jk
Keywords: ATO-Ag hybrid electrode, Transparent conductive oxide, ATO, Thermal roll imprint, Sol coating, Ag metal grid
DOI: 10.3938/jkps.68.779

I. INTRODUCTION

Recently, transparent conducting electrode substrates have been widely used and their applications have greatly being increased greatly due to the growth of the display and the solar cell industries. In general, transparent conducting electrodes require high electrical conductivity (below 10^{-3} Ω/cm) and high optical transmittance (80%) at visible wavelengths [1]. These conditions are essential requirements if the electrodes are to be applied to optoelectronic devices [2,3]. For these reasons, currently, various materials are being applied as substrate materials for transparent conductive electrode; these materials include metals, metallic oxides, conductive polymers and carbon materials [4,5]. Especially, metallic thin films are not adequate as transparent electrodes due to the their low transmittance at the visible wavelengths, in spite of the in high conductivity. In addition, conductive polymers and carbon materials need more researches to reach commercialization because of their high sheet resistance and low transmittance.

The most widely used transparent conductive material is indium tin oxide (ITO) [5,6]. Due to the growth of the display industry and the solar-cell market, high-quality, transparent, conducting electrodes that are printable and flexible have been receiving more attention. However, ITO thin films are not appropriate for was as flexible, transparent, conducting oxide substrate, because they lack flexibility and expensive [7, 8]. Especially, when doped metal- oxide thin films are bent or folded, their electrical conductivity deteriorates due to its poor mechanical properties [9]. In addition, ITO thin films need an annealing process at a high temperature over 300 °C to get high transparency and low resistance. This process requires expensive vacuum equipment, which, in turn, increases the material cost, which increases the cost of fabricating indium-tin-oxide thin films [10]. As a solu-

*E-mail: yaliyali3@hanmail.net

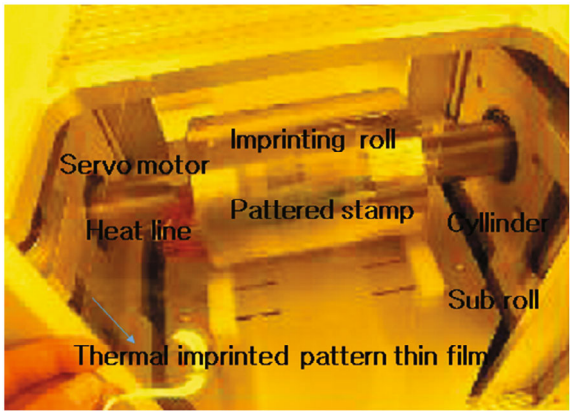

Fig. 1. (Color online) Apparatus for thermal roll imprinting and PET roll on which mesh patterns will be imprinted.

tion to the problems with ITO thin films, hybrid electrodes made of a patterned metal grid and a conducting transparent oxide have been studied due their low sheet resistance and flexible characteristics [11]. According to the literature, hybrid types of electrodes with Ag grids have high transparency (82%) and a lower sheet resistance than general transparent electrode [12]. Although a metal-grid -based transparent electrode has been reported and manufactured due to its many advantages,research on hybrid electrodes with Ag grids and define antimony tin oxide that are fabricated by keeping a thermal-roll imprinting (TRI) method is still lacking.

This paper suggests a new hybrid electrode that is fabricated for use in flexible displays by using the TRI method followed by wet coating. We also report the characteristics of the Ag/ATO hybrid transparent electrode. This simple process can be applicable for mass production through the roll-to-roll process. We were able to form a transparent hybrid electrode a with low resistance and a high transmittance at room temperature without any kind of vacuum equipment.

II. EXPERIMENTAL PROCEDURES

1. Materials for the Transparent Electrode Film

The substrate used for the experiment were polyethylene terephthalate (PET) (MSK 3100), which is flexible plastic film with a 100 μm thickness. According to measurements of the properties of the PET Film, transmittance was above 90%, and its haze was about 0.5% with a T_g of 130 °C. The silver paste used had a 70% silver content, a viscosity of 10,000 cps and a specific resistivity of 1×10^{-5} Ω/cm. The silver paste which contained several hundred nano-particles was made by Inktec Co., Ltd (Korea).

We used ATO sol-solution materials to obtain the hybrid thin film because their product cost is much lower than the cost of an ITO sol solution and other Transparent Conductive Oxide materials such as a Carbon Nano Tube sol, a polymer sol and so on. In addition, antimony -tin- oxide films are attractive due to their unique physical properties, such as their high transparency in the visible region and their high reflectivity in the infrared region. Thus, they can be used in to the optoelectronic devices such as hybrid microelectronics and for solar-energy applications. In addition, ATO films exhibit the very good property and chemical stability and have good mechanical durability and superior adhesion to substrates [13]. Antimony-doped tin-oxide films (ATO, SnO_2:Sb) were prepared with a 0.2-M solution of $SnCl_2$ in ethanol with the addition of 5-mol% $SbCl_3$ and 0.4-M DAA (di acetone alcohol, 4-hydroxy-4-methyl-2-pentanone) as a stable agent. The solid content of the ATO suspension was 30 wt%, and its suspension was stirred by using a magnetic stirrer for 1 hour.

2. Experimental Equipment

In order to fabricate an electrode thin film with low resistance and high optical transparency, We used the thermal roll imprinting (TRI) method. The method has the advantages of better uniformity, less loading pressure, simple structure and low cost compared to the semiconducting process. Figure 1 shows the apparatus for thermal roll imprinting of ATO/Ag hybrid electrodes. The appareturs a thermal imprinting system with a heating roll and an imprinting roll on which the patterns are fabricated by the Korea Institute of Machinery and Materials (KIMM) on request. The flexible stamp mold was fabricated by electroforming a nickel and cobalt alloy to dimension of 250 × 250 mm^2. A flexible mold of about 200 μm in thickness was mounted on a heating roll using two roll click gears, as shown in Fig. 2(b). The stamp mold was a grid mesh made of rails, 10-μm wide and 10-μm high with a 510-μm pitch, and was applied to the transparent conducting thin films with areas of 10 × 10 mm^2. The cartridge heater of the heating roll was used to control the temperature for temperature up to 200 °C. Figure 2(c) shows the TRI system with a heating roll and an imprinting roll. The latter was coated with Cr to avoid scratching the polymer film. The rolls with line-to-line contact could exert a maximum force of 550 kgf via a servo motor. The imprinted micro-scale channel patterns were directly filled with nano-paste by using the doctor blade method, as shown in Fig. 2(e). After that, heat treatment was applied in a drying furnace at a temperature of 120 °C for 10 minutes. then, the ATO solution was coated on the PET film by using the doctor blade method. The ATO/Ag thin film layer's thickness was changed by varying the doctor blade's speed and the blade's height. then, annealing was performed for 10 minutes at 120 °C as shown in Fig. 2(f) − (h). Finally, the roll-cleaning process was performed to remove the

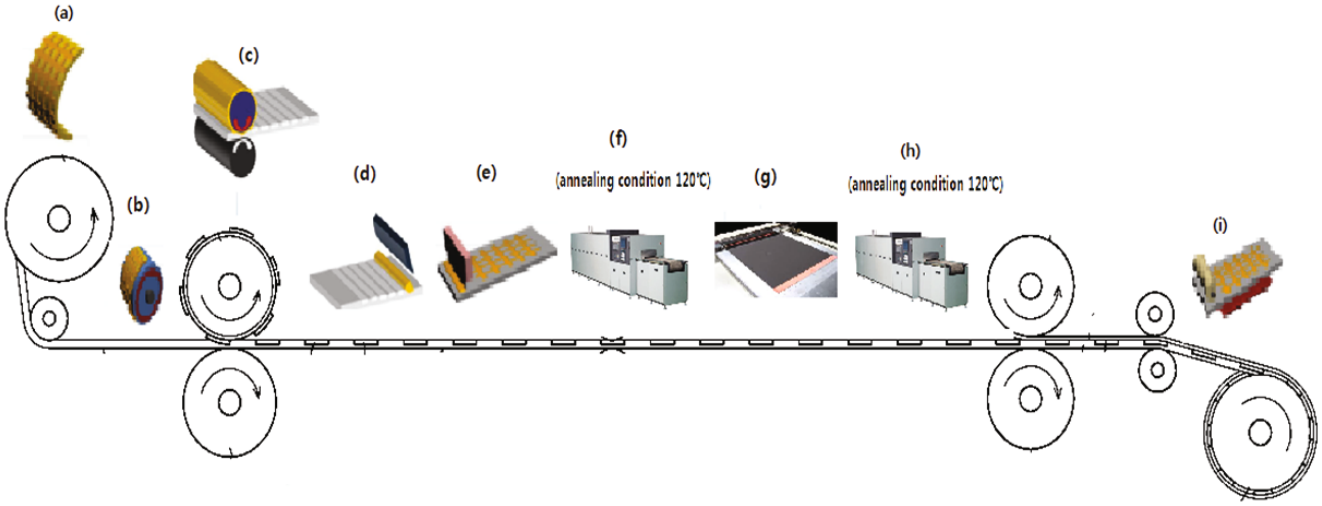

Fig. 2. (Color online) Schematic diagrams of the fabrication process for embedded type TCF: (a) fabrication of a flexible stamp mold, (b) wrapping the stamp mold on the thermal roll, (c) high-resolution roll imprinting on a polymer film, (d) dropping of conductive Ag nano-paste on the patterned film, (e) doctor blading of the Ag nano-paste, (f) annealing of the Ag nano-paste at 120 °C, (g) ATO sol coating by using the doctor blade method, (h) annealing of the ATO film at 120 °C and (i) roll cleaning and drying of the Ag/ATO film.

rest of Ag paste on the surface of the film. The films with Ag paste embedded were annealed at 140 °C for 5 minutes in a near-infrared (NIR) drying system, which resulted in the fabrication of ATO/Ag grid hybrid-type transparent electrodes.

3. Characterizations

The thicknesses of the ATO/Ag hybrid thin films were measured by using a surface profiler (alpha-step: TENCOR 500). The optical transmittance spectra of the ATO/Ag hybrid thin films were measured by using a UV-visible spectrometer (UV-3150, Shimadzu, Japan) in the visible wavelength range of 200 − 800 nm. The crystalline structures of the ATO/Ag hybrid thin films were characterized by using an X-ray diffractometer (XRD: Bruker, AXS D8). The sheet resistance was measured by using a four-point probe (Chang Min Co. Ltd., Korea). Field-emission scanning electron microscopy (FE-SEM: JEOL-7401F) and atomic force microscopy (AFM: Park Scientific Inc.) were used to examine the surface morphologies. Finally, bending tests were performed using bending test equipment (ZBT: 200, Zitec Co., Korea).

III. RESULTS AND DISCUSSION

Figure 3 shows the XRD patterns of the ATO/Ag hybrid thin films fabricated with different film thicknesses by using the doctor blade method. With increasing thickness of the ATO/Ag hybrid thin films, the XRD

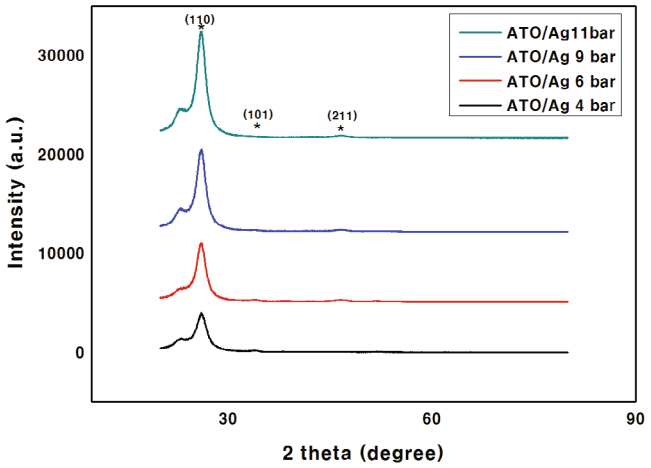

Fig. 3. (Color online) X-ray diffraction patterns of ATO/Ag hybrid thin films with different thicknesses.

peak became stronger and sharper. In addition, the XRD pattern indicated a crystalline structure for the ATO/Ag hybrid thin films, sharp crystallization peaks being located at the (110) orientation and small broad peaks at the (101), and the(211) orientations. However, the (112), (200) and (301) diffraction peaks did not appear [14]. A strong peak is located at approximately 26.76°,indicating that the preferred orientation is the (110) plane [15].

The above trends have been reported in many articles by several researchers [16, 17] and show that the (110) orientation plane has the lowest surface free energy in the ATO thin film. This is due to the (110) orientation being related to the presence of oxygen vacancy defects within the ATO lattice, which is connected with increases

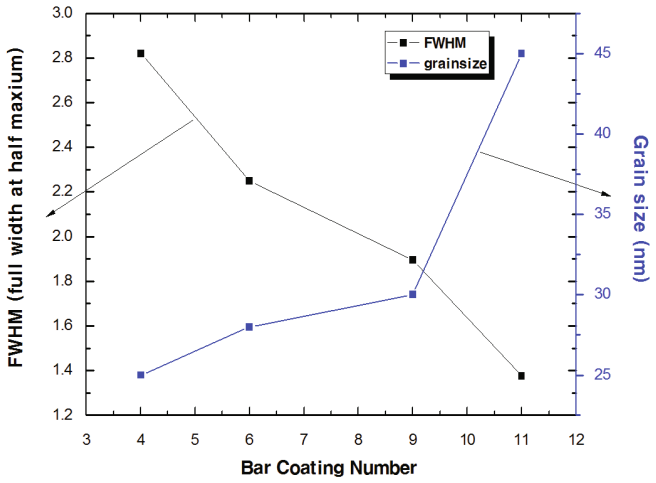

Fig. 4. (Color online) FWHM and grain size of Ag/ATO thin films as functions of the bar coating number after annealing at 120 °C.

in the charge carrier concentration and the grain size [18]. In addition, other peaks with smaller intensities are located at approximately 34.27° and 46.8°, and can be identified as being due to the (101) and the (211) planes, respectively. This is influenced by the grain boundary energy and by the diffusion of surface atoms, potentially [19, 20]. In addition, no peak associated with the was found because the ATO thin film layer covered the Ag grid line and most of the region between Ag grids. All the diffraction peaks were in good agreement with reflection due to the cassiterite ATO phase (JCPDS card No. 88-2348) [21].

In order to evaluate the crystallinity of the ATO/Ag hybrid thin films, we investigated the full width at half maximum (FWHM), and are calculated and the grain size from the XRD Peak's spectra by using the Scherrer's equation [22]:

$$D_{grain} = 0.94\lambda/\beta\cos(\theta_B). \quad (1)$$

where D_{grain} is the size of a crystal grain, β is the broadening of the diffraction line measured at half width maximum intensity in radians of the XRD peak associated with the (110) plane, λ denotes the wavelength of the used CuK_α line (0.154 nm) and θ_B denotes the Bragg diffraction angle.

Figure 4 shows the grain-size and the full-width at half-maximum (FWHM) data for the (110) orientation in the ATO/Ag hybrid thin film, As the thickness of the ATO/Ag thin film was increased, the grain size increased, and the peak associated with the (110) became more intense and sharper, which resulted in an improvement of the crystal quality [23].

Figure 5 shows the SEM images of the surface morphologies and Ag nano-particles and the empty channels of 5.1 μm in width and 4.2 μm. in depth that were thermally imprinted on the PET. In this processing, PET thin films were thermally imprinted at 100 °C under 200 kgf at a speed of 15 mm/sec in the depth of the channel. Figure 5(a) − (c) shows the SEM images of the Ag grid lines with widths of 5.1 μm and pitches of 250 μm; the thickness of an Ag grid line was around 4.2 μm. From the SEM image in Fig. 5(c), we can see that the excellent filling of the narrow channels had been realized basically by the application of a water- based nano-sized silver paste on a hydrophobic PET substrate. The Ag particles had sizes between 20 nm and 150 nm, which was small enough to accomplish compact packing in the patterned line.

The narrow grid line channel and the nano-particles played important roles in the electrical properties and made it possible to produce at large-scale roll-to-roll process. The process for embedding metal grids required an additional fabrication step in the channel to obtain a TCO thin film. In order to provide sufficient conductivity between the silver grid lines and the ATO thin film, we used the doctor blade coating method to coat the ATO thin films. In order to optimize the hybrid TCO thin film, We used the ATO sol solution and the bar coating method to produce Films with various thicknesses, and the thickness of the thin film was measured using a surface profiler. The layer thickness of the ATO/Ag thin film could be varied between 0.2 μm and 0.8 μm, different sheet resistances and different optical transmittances could be obtained.

Because of the strong bonding between the ATO layer and the Ag particles a denser and stronger network is expected, which, in turn, has an effect on the electrical properties of the ATO/Ag hybrid thin films. Figure 6 shows the morphologies of ATO thin film surfaces annealed at 120 °C. The ATO thin films had a nanostructure, and the Ag grid of ATO with 5 μm pattern lines was covered by the ATO thin film. With increasing ATO/Ag hybrid thin-film thickness, the ATO grains were agglomerated. This phenomenon can be explained as follows: the numbers of oxygen vacancies and the antimony's defects were reduced with increasing grain size. This agrees well with the XRD results shown in Fig. 3 and with Lee et al's results [24]. According to their results, compressive stresses in the films affect the recrystallization and grain growth, which leads to increase d conductivity.

When the Ag/ATO thin film's thickness was increased, the film gradually exhibited grain growth, Because the thermal energy of the crystallization was spent for grain growth, and the grains were arranged in a way to ensure a low surface energy. That contributed to the improved crystallization and grain growth in the thin film and, subsequently, improved the physical properties of the transparent electrode. In this study, crystal growth played an important role in the ATO/Ag thin film, and the film's microstructure affected the optical and the electrical properties.

In order to understand the surface morphologies of the ATO/Ag grid thin film layers, we measured the RMS roughness by using the AFM equipment. With increas-

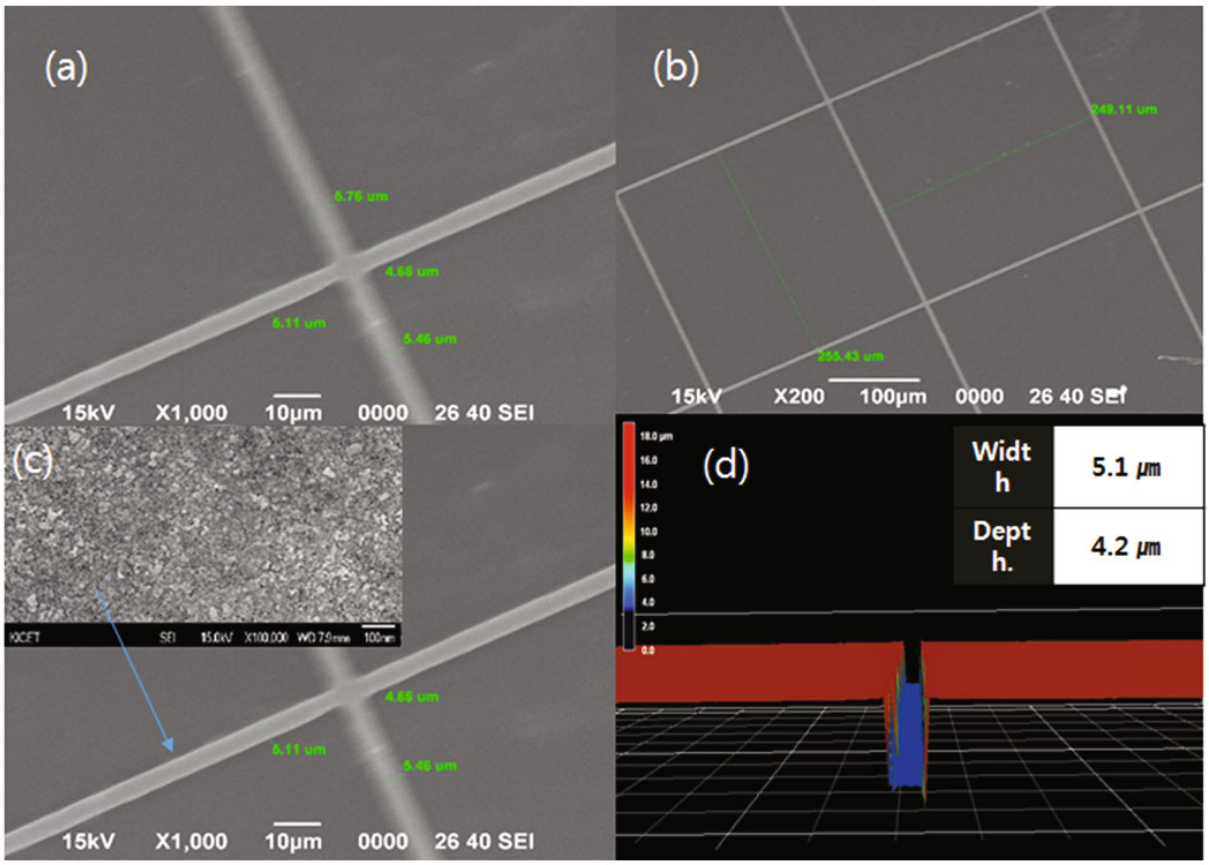

Fig. 5. (Color online) Top: FE-SEM images of (a) PET foil a with silver grid pattern line, (b) pitch between lines, (c) Ag nano-particles, and (d) 3-dimensional cross section of image of the PET foil before silver pattern application.

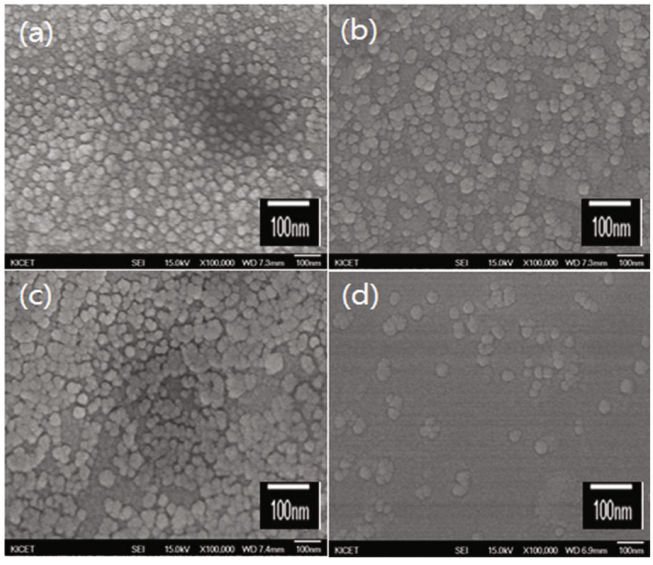

Fig. 6. SEM images of the ATO/Ag thin films with different coating thicknesses coated by using the (a) No. 4, (b) No. 6, (c) No. 9 and (d) No. 11 bar.

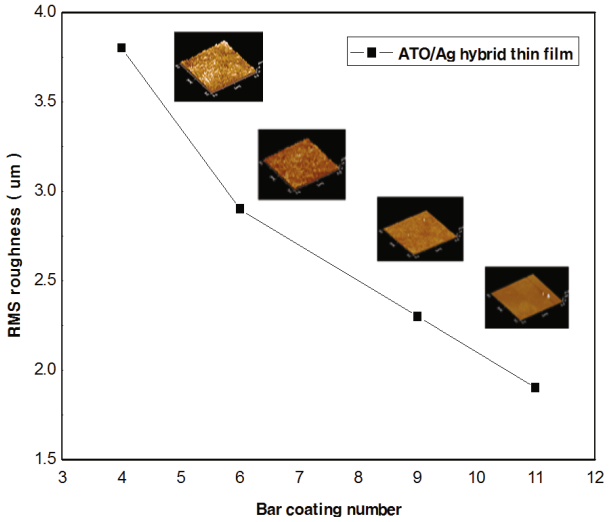

Fig. 7. (Color online) AFM Images of Ag/ATO thin film layers coated by using the (a) No. 4, (b) No. 6, (c) No. 9 and (d) No. 11 bar.

ing ATO/Ag grid film thickness, the surface morphologies changed as shown in Fig. 7. The AFM images revealed that the average size of the particles increased

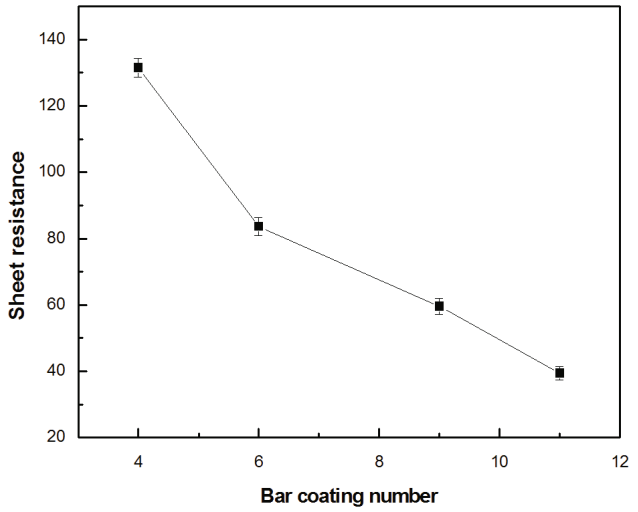

Fig. 8. Change in the resistance of the ATO films with changing bar coating after heat treatment at 120 °C.

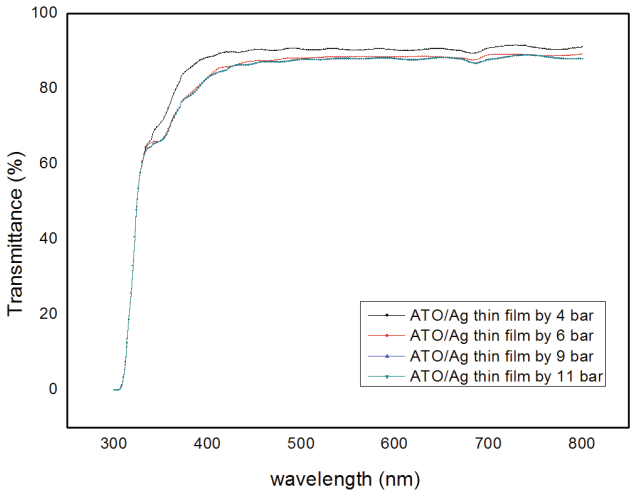

Fig. 9. (Color online) Variations Optical Transmittances at 550 nm with respect to PET films with Various thicknesses that had been heat treated at 120 °C.

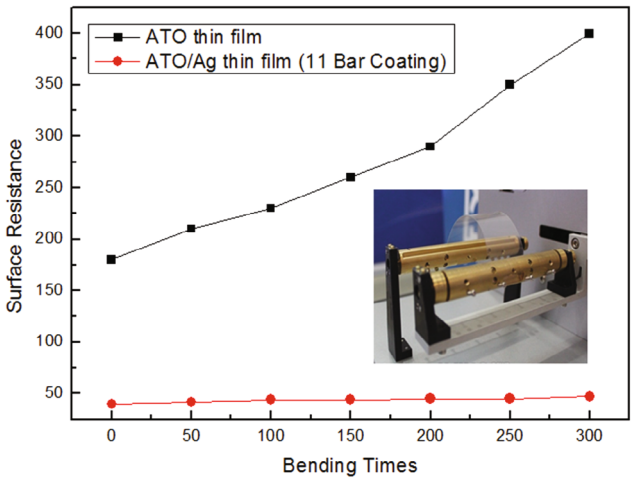

Fig. 10. (Color online) Bending test results for ATO and for the ATO/Ag hybrid electrode grown on a PET substrate.

with increasing film thickness of the ATO/Ag grid thin film. Also, the surface roughness decreased with increasing thickness of the ATO/Ag thin film. This is one of the important reasons for using an embedded channel line in the hybrid thin films because the thermal imprinting method leads to uniform film thickness in the ATO/Ag grid thin films. The crystal quality and morphology are well known to important factor in the film [25]. and the AFM morphologies agreed well with the FE-SEM results shown in Fig. 4.

Figure 8 shows the sheet resistance in the ATO/Ag thin film and it depends on the thin film's thickness after the annealing treatment. With increasing ATO/Ag thin film thickness, its sheet resistance varied from 41 Ω/sq to 220 Ω/sq. This agrees with the research result that the sheet resistance decreases as the thin-film's thickness increases and the grain size increase. Therefore, the annealing treatment affected the microstructure, and atoms were redistributed to more stable positions to reach thermal equilibrium inside the film. Numerous types of defects, such as vacancies, interstitials and impurities, are located in the ATO/Ag hybrid thin film, and they are related to the change s in the equilibrium concentration [26].

Figure 9 shows the optical transmittance in the visible region for ATO/Ag thin film with thickness from 0.2 μm to 0.8 μm in 0.2-μm intervals. In the visible wavelength range, the average optical transmittance were over 80% after annealing at 120 °C. The optical transmittance is closely related to the surface structures, film's thickness, the grain size and so on. A small grain size and a rough surface morphology decrease the optical transmittance due to increased optical absorption and surface scattering. The ATO/Ag thin films had high transmittances under the No. 11 bar coating condition, which is due to the increased grain size and the decreased scattering on the surface because of the decreased numbers of grain boundaries and defects in the ATO/Ag thin film [27]. Consequently, the fabricated ATO/Ag mesh electrodes showed a high optical transmittance of about 85.31% in the visible wavelength and a sheet resistance of the 41 Ω/sq. under the No. 11 bar coating condition.

Figure 10 shows the results of the bending tests in the ATO and the ATO/Ag hybrid thin films on PET substrates. The ATO/PET sample and the ATO/Ag grid sample were coated with a 100 × 100 mm^2 size. The head speed of the bending tester was 160 mm/sec, and the number of the total bending tests was 300 cycles. In order to analyze the mechanical properties of the ATO and the ATO/Ag thin films, we measured the electrical properties by using a 4-point probe after 50 cycles of the bending test. With increasing number of cycles of the bending test, the resistance of the ATO thin film increased, which was related to the formation of micro-

cracks [28].

An increase in the resistance has a strong effect on the efficiency in a flexible solar cell and the lifetime of flexible optoelectronic devices such as Organic lighting emitting diodes (OLED). However, in case of an ATO/Ag hybrid thin film, its resistance was maintained at about 41 Ω/sq even after 300 cycles of the bending test, indicating that the resistance had not changed. The Ag grid nano-layer deposited by using the doctor blade method played an important role as a buffer layer to improve adhesion between the ATO thin film layer and the PET substrate. At the same time, the Ag grid could reduce the physical stress caused by the bending test. As a result the bending test, confirmed that the ATO/Ag hybrid film could be applied as a substrate for optoelectronic devices. Finally, the ATO/Ag hybrid thin film contributed to improving the efficiency and the lifetime of the flexible devices like define DSSCs, or OLEDs.

IV. CONCLUSION

In summary, in order to replace ITO transparent electrodes, we fabricated a hybrid transparent electrode made of an ATO thin film coated by bar-coating and an Ag grid by thermal-roll imprinting (TRI); low-temperature silver paste was filled into the TRI patterns by using through the doctor blade (DB) method. The sheet resistance was lowered to 40 Ω/sq by applying a silver-paste mesh pattern with a 5 μm line width and a 250 μm line separation. This methodology may be a possible candidate for fabricating transparent electrodes that are characterized by a low sheet resistance and a high transparency due to the large opening between the silver lines. Because this method has a low process temperature, and is lower number of processes, it may provide a scalable and lower cost method for fabricating transparent electrodes than the PVD process for fabricating than oxide films.

Furthermore, bending test results showed that the R2R grown ATO/Ag thin film had good flexibility, indicating its applicability to flexible displays and solar cells.

REFERENCES

[1] A. Tracton, *Coatings Technology Handbook*, Thrid Edition Marcel Dekker (2005).

[2] T. Minami, Semicond. Sci. Technol. **20**, 35 (2005).

[3] H. Kim, C. M. Gilmore, A. Pique, J. S. Horwitz, H. Mattoussi, H. Murata, Z. H. Kafafi and D. B. Chrisey, J. Appl. Phys. **86**, 6451 (1999).

[4] J. Y. Lee, S. T. Connor, Y. Cui and P. Peumans. Nano Lett. **8**, 689 (2008).

[5] M. J. Keum and J. G. Han, J. Korean Phys. Soc. **53**, 1580 (2008).

[6] S. De, T. M. Higgins, P. E. Lyons, E. M. Doherty, P. N. Nirmalraj, W. J. Blau, J. J. Boland and J. N. Coleman, ACS Nano. **3**, 1767 (2009).

[7] H. Hosono, H. Ohta, M. Orita, K. Ueda and M. Hirano, Vacuum **66**, 419 (2002).

[8] K. Alzoubi, M. M. Hamasha, S. Lu and B. Sammakia, J. Disp. Technol. **7**, 593 (2011).

[9] H. K. Yu, S. Kim, B. Koo, G. H. Jung, B. Lee, J. Ham and J. L. Lee, Nanoscale **4**, 6831 (2012).

[10] S. R. Forrest. Nature **428**, 911 (2004).

[11] M. G. Kang and L. J. Guo, Advanced Materials **19**, 1391 (2007).

[12] J. Zou, H. L. Yip, S. K. Hau and A. K. Y. Jen, Appl. Phys. Lett. **96**, 203301 (2010).

[13] B. Benrabah, A. Bouaza, A. Kadari, M.A. Maaref, Super lattice Microstruct. **50**, 591 (2011).

[14] F. J. Berry and C. Greaves, J. Chem. Soc. Dalton Trans. **12**, 2447 (1981).

[15] B. Stjerna, E. Olsson and C. G. Granqvist, J. Appl. Phys. **76**, 3797 (1994).

[16] K. Suzuki and M. Mizuhashi, Thin Solid Films **97**, 119 (1982).

[17] C. Korber, J. Suffner and A. Klein, J. Phys. D: Appl. Phys. **43**, 29 (2010).

[18] J. Montero, C. Guillén and J. Herrero, Solar Eng. Matter Solar Cells. **95**, 2113 (2011).

[19] H. Kim and A. Pique, Appl. Phys. Lett. **84**, 218 (2004).

[20] W. Bergermayer and I. Tanaka, Appl. Phys. Lett. **84**, 909 (2004).

[21] F. J. Berry and C. Greaves, J. Chem. Soc. Dalton Trans. **12**, 2447 (1981).

[22] T. Trindade, P. O'Brien and NL Pickett, Chem. Mater. **13**, 3843 (2001).

[23] A. Eshaghi and A. Graeli, Optik **125**, 1478 (2014).

[24] Y. C. Lee, S. Y. Hu, W. Water, Y. S. Huang, M. D. Yang, J. L. Shen, K. K. Tiong and C. C. Huang, Solid State Comm. **143**, 250 (2007).

[25] A. Mansingh and C. V. R. Vasant Kumar, J. Phys. D: Appl. Phys. **28**, 1448 (1995).

[26] M. Kojima, H. Kato and M. Gallo, Philosophical Magazine B **73**, 289 (1996).

[27] A. Eshaghi, M. Pakshir and R. Mozaffarinia, Appl. Surf. Sci. **256**, 7062 (2010).

[28] D. R. Cairns, R. P. Witte II, D. K. Sparacin, S. M. Sachsman, D. C. Paine, G. P. Crawford and R. R. Newton, Appl. Phys. Lett. **76**, 11 (2000).